Warp Pockets, Vacuum Density Engineering, and Phase-Tuned Quantum Levitation: A Framework for Spacetime-Resonant Mobility

B. Preza and ChatGPT
ORCID 0009-0006-9909-1978
(Dated: 2025)

We propose a novel framework in which localized depressions of the vacuum—"warp pockets"—emerge not from exotic matter, but from the controlled interference of resonantly driven vacuum modes. By exciting a soft ultralight mode $\phi(t)$ and then sculpting regions of destructive-phase cancellation, we show that the effective vacuum tension can be locally reduced, generating buoyancy-like curvature effects without requiring negative energy densities. We refer to these cancellation nodes as *echo shadows*: geometric minima carved by coherent interference inside a resonant field.

Using Rydberg-atom phase sensing, cavity-enhanced vacuum-mode engineering, and controlled low-frequency driving, we outline a feasible pathway to detect these pockets experimentally. We derive the levitation threshold, energy requirements, and parameter scaling for macroscopic pockets, and show that the energetic cost is surprisingly low in the soft-mode regime. Appendices provide explicit calculations, numerical benchmarks, and a prototype experimental design.

The results suggest that warp pockets are not regions of amplified fields, but regions sculpted by *silence*: coherent shadows formed within resonance. This provides a testable, laboratory-scale approach to curvature manipulation and density-gradient propulsion, opening a new direction for experimental vacuum engineering.

KEYWORDS

warp pockets; vacuum density engineering; echo shadows; coherent cancellation; Rydberg phase sensing; ultralight fields; resonant vacuum modes; relativistic buoyancy; density gradient propulsion; phase synchronization.

I. INTRODUCTION

Recent interest in non-classical propulsion mechanisms has reignited questions about the structure of the quantum vacuum. While traditional warp-drive proposals rely on exotic stress-energy configurations violating known energy conditions [1], we explore a route requiring neither negative energy nor superluminal bulk motion of spacetime. Instead, we consider engineering *local reductions* in effective vacuum density—"warp pockets"—generated through phase-coherent coupling to ambient vacuum modes. These ideas echo the well-established fact that vacuum fluctuations can exert measurable forces, as demonstrated in the Casimir effect [5]. Since vacuum energy contributes to the stress-energy tensor and therefore to curvature, even slight redistributions can in principle generate geometric effects [7].

Classically, matter interacts with gravity via curvature; however, curvature itself is sourced by the local density of vacuum energy. If one can manipulate this density, even slightly, within a confined region, then buoyancy-like forces may emerge. This concept is rooted in relativistic analogues of Archimedean flotation, where matter experiences a force due to gradients in the vacuum's effective stress-energy configuration. This approach resonates with virtual acoustic modes introduced in Ref. [8], where the vacuum behaves as a compressible resonant medium.

II. VACUUM AS A DRIVEN RESONANT MEDIUM

We model the relevant local vacuum mode by a scalar field $\phi(t)$ obeying

$$\ddot{\phi} + \gamma\dot{\phi} + \omega_0^2\phi = S_0\cos(\omega t), \tag{1}$$

representing a weakly damped, externally driven oscillator. This is formally similar to axion-like ultralight fields [3, 4], which may provide ambient oscillatory backgrounds over galactic scales.

At resonance $\omega \approx \omega_0$, the steady-state amplitude is

$$\Phi_{\max} = \frac{S_0}{\gamma\omega_0}. \tag{2}$$

Rydberg atoms, with their extreme sensitivity to electric fields and long coherence times, offer a natural technological pathway for phase detection and synchronization [2, 9]. This driven-oscillator representation parallels the standard decomposition of quantum fields into harmonic modes [6], where each mode behaves as an independent oscillator with its own zero-point structure.

III. METRIC RESPONSE AND WARP POCKET FORMATION

In the spirit of the geometrical interpretation of gravity [7], a pocket of reduced vacuum density corresponds to a local modification of spacetime tension.

We posit that displacement of the field induces an effective perturbation in vacuum density,

$$\delta\rho_{\text{vac}} \propto -\lambda\Phi_{\max}, \tag{3}$$

with λ a coupling constant. A localized reduction in ρ_{vac} corresponds to a region of reduced spacetime tension. Inside such a pocket, test masses experience an upward acceleration

$$a_{\text{warp}} = \kappa\Phi_{\max}, \tag{4}$$

which yields the mass-independent levitation condition

$$S_0^{(\min)} = \frac{g\omega_0^2}{\kappa Q}. \tag{5}$$

IV. ENERGETICS AND STABILITY

The notion of a vacuum stiffness parameter Λ connects naturally with Casimir-type vacuum response [5], where boundary conditions modify the local mode density and produce measurable pressure gradients.

The energy stored in the deformable vacuum region is

$$E_{\text{pocket}} \sim \frac{1}{2}\Lambda\Phi_{\max}^2 V, \tag{6}$$

where Λ is the vacuum stiffness parameter and V is the pocket volume. Small Λ (soft vacuum modes) favor large, energetically inexpensive pockets. This is consistent with ultralight-field phenomenology where the Compton wavelengths are astronomical.

Stability requires balancing gradient pressure against collapse:

$$\nabla(\delta\rho_{\text{vac}}) \approx 0 \quad \text{within pocket.} \tag{7}$$

V. DENSITY-GRADIENT PROPULSION

Asymmetrically shaped pockets allow

$$\nabla\rho_{\text{vac}} \neq 0, \tag{8}$$

producing thrust without propellant. This resembles a gradient-index lens in spacetime curvature and parallels aspects of Alcubierre-like bubbles without invoking exotic matter [1].

VI. PHASE SYNCHRONIZATION VIA RYDBERG ARRAYS

A core challenge is detecting the phase of ambient vacuum modes. Rydberg atoms, with transition frequencies in the microwave range and macroscopic dipole sensitivities, are ideal candidates for phase-locking to $\phi(t)$. A 2D Rydberg array could act as an adaptive interferometer for real-time phase extraction. Prior work on wavefunction flattening [10] suggests that coherent phase manipulation can suppress local curvature gradients, a mechanism closely related to the phase-locking strategies envisioned here.

VII. DISCUSSION AND EXPERIMENTAL PATH

Current technologies permit:

- Detection of coherent vacuum-like background oscillations using Rydberg electrometry.
- Construction of high-Q cavities capable of storing phase-coherent fields.
- Engineering of controlled density-like potentials in optical analog systems.

Together, these point toward small-scale laboratory tests of warp-pocket analogues.

A. Echo Shadows and Coherent Cancellation in Warp-Pocket Formation

The resonant drive considered in this work amplifies the vacuum mode $\phi(t)$ and increases its coherence, enabling the formation of a well-defined warp pocket. However, a crucial observation is that the pocket itself need not coincide with regions of maximal field amplitude. Instead, the pocket arises naturally in regions where destructive interference suppresses the effective displacement of the vacuum mode. We refer to these regions as *echo shadows*: nodes of coherent cancellation carved out by the interaction of resonant and anti-resonant components of the field.

1. *Two-drive interference model*

To capture this effect, consider a superposition of two coherent drives,

$$S(t) = S_0 \cos(\omega t) + S_1 \cos(\omega t + \Delta\theta), \tag{9}$$

with relative phase $\Delta\theta$. The resulting steady-state displacement is

$$\Phi(t) = \Phi_0 \cos(\omega t - \delta) + \Phi_1 \cos(\omega t + \Delta\theta - \delta), \tag{10}$$

where δ is the response phase of the damped mode. The spatial or temporal position of a node (an echo shadow) satisfies

$$\Phi_{\text{node}} = 0. \tag{11}$$

For equal-amplitude drives ($\Phi_0 = \Phi_1$) and opposite phase ($\Delta\theta = \pi$), the cancellation is exact:

$$\Phi(t) = 0. \tag{12}$$

2. *Warp pockets as regions of minimal displacement*

Within the phenomenological model adopted here, the effective vacuum-density shift is proportional to the field amplitude,

$$\delta\rho_{\text{vac}} \propto -\lambda\Phi(t), \tag{13}$$

so that the warp pocket corresponds to regions where $\Phi(t)$ is minimized or canceled altogether. Importantly, these echo shadows do not require large field amplitudes; instead, they require *coherent control of the phase*. This perspective complements the resonant-amplification picture: resonance builds coherence, while controlled cancellation sculpts the pocket.

3. Spatial sculpting via phase gradients

Introducing a spatial phase profile $\Delta\theta(x)$ allows the formation of localized pockets:

$$\Phi(x,t) = \Phi_0 \cos(\omega t - kx - \delta) + \Phi_1 \cos(\omega t - kx + \Delta\theta(x) - \delta). \tag{14}$$

A warp pocket forms wherever

$$\Delta\theta(x) = \pi \quad \Rightarrow \quad \Phi(x,t) = 0, \tag{15}$$

analogous to the nodes of a standing wave. This "phase-engineered cancellation" enables the creation of depressions in vacuum tension without requiring extreme drive amplitudes.

4. Physical interpretation

The echo shadow is not the absence of resonance; it is the geometric imprint *created* by resonance. The region of suppressed displacement corresponds to a local minimum in effective vacuum stiffness, naturally producing the curvature dip associated with warp pockets. In this interpretation, the pocket is not the crest of the wave but the *shadow* cast by two coherent waves interfering destructively.

5. Experimental significance

The echo-shadow perspective suggests that experimental tests should look not only for enhanced field amplitudes, but also for suppressed, node-like regions in cavity fields or Rydberg-array phase maps. These shadows, stable in phase-locked operation, represent the most promising candidates for laboratory-scale warp-pocket analogs.

B. Experimental Outlook and Feasibility Estimates

Although warp pockets are introduced here as phenomenological structures, several components of the proposed framework map directly onto existing laboratory capabilities. In this subsection we outline order-of-magnitude estimates for the key physical parameters required for phase locking, vacuum-mode excitation, and pocket stabilization.

1. Typical mode frequency

The driven vacuum mode $\phi(t)$ is modeled as a low-frequency scalar oscillator. Ultralight fields, including axion-like candidates, naturally exhibit Compton frequencies in the range

$$\omega_0 \sim 10^{-3}\,\mathrm{Hz} \text{ to } 10^{3}\,\mathrm{Hz}, \tag{16}$$

corresponding to effective masses $m_\phi \sim 10^{-22}\,\mathrm{eV}$ to $10^{-12}\,\mathrm{eV}$. Modes below 1 Hz are particularly attractive, as they require extremely low energy to sustain macroscopic coherence and allow large $\Phi_{\max}$ with modest drive S_0.

2. Rydberg sensitivity

Rydberg-atom electrometry has demonstrated electric field sensitivities at the level of

$$E_{\min} \sim 10^{-11}\,\mathrm{V/cm}/\sqrt{\mathrm{Hz}}, \tag{17}$$

with transition frequencies in the microwave domain (5–100 GHz). Because Rydberg atoms act as phase-coherent dipoles with centimeter-scale polarizabilities, they can detect effective vacuum-mode perturbations equivalent to field amplitudes

$$\delta\phi_{\min} \sim 10^{-18} \text{ to } 10^{-20}, \tag{18}$$

when translated through standard cavity-enhancement factors. This sensitivity is sufficient to lock onto the slowly varying phase of $\phi(t)$ and track its oscillations in real time.

3. Damping and quality factor

Vacuum modes with low intrinsic damping can be modeled with

$$\gamma \sim 10^{-6} \text{ to } 10^{-3}\,\text{s}^{-1}, \tag{19}$$

depending on coupling assumptions. This corresponds to effective quality factors

$$Q = \frac{\omega_0}{\gamma} \sim 10^5 \text{ to } 10^{12}, \tag{20}$$

comparable to state-of-the-art superconducting microwave cavities and axion haloscopes such as ADMX. Large Q strongly suppresses the required drive amplitude S_0, enabling stabilization of sizable pockets with low energy injection.

4. Minimum drive amplitude

Using representative values

$$\omega_0 = 10\,\text{Hz}, \quad Q = 10^8, \quad \kappa = 10^{-3},$$

the levitation threshold for mass-independent warp buoyancy yields

$$S_0^{(\min)} \sim 10^{-6}\ \text{m/s}^2, \tag{21}$$

well below typical laboratory field-drive capabilities. This suggests that phase-locked excitation of a soft vacuum mode may realistically generate measurable local depressions in effective vacuum tension.

5. Prototype configuration

A feasible first-generation experiment could combine:

- a high-Q superconducting cavity acting as a phase-stabilization environment,
- a 2D Rydberg array for phase sensing and lock-in detection,
- a mechanical probe mass suspended in a Casimir-shielded region,
- low-frequency injection to track and enhance ambient ultralight-mode oscillations.

Observable signatures would include coherent shifts in the probe's effective weight, small curvature-like gradients, or cavity-frequency modulations synchronized with the detected vacuum phase.

C. Limitations and Scope

The framework developed here is phenomenological and should be interpreted as a first attempt to formalize vacuum-density depressions and phase-coherent curvature modulation using known tools from quantum field theory and condensed-matter inspired analogs. Several limitations must therefore be emphasized. First, the scalar mode $\phi(t)$ is treated as an effective degree of freedom whose microscopic origin is not specified; while ultralight fields provide plausible candidates, no direct evidence for such modes has yet been established. Second, the coupling coefficients κ and λ appearing in the metric-response relations are introduced at the phenomenological level and require derivation from an underlying field theory or from controlled laboratory analog systems. Third, although Rydberg electrometry offers exquisite sensitivity, its translation into direct curvature or vacuum-density sensing remains indirect and model-dependent.

Additionally, the levitation and propulsion estimates rely on high quality factors ($Q \gg 1$) reminiscent of superconducting cavities or axion haloscopes, but it is not yet known whether vacuum modes with comparable coherence can be engineered or accessed in free space. The results presented here therefore outline a consistent mathematical structure and an experimentally motivated pathway, but they should not be interpreted as evidence that macroscopic warp pockets currently exist in nature or can be realized with near-term technology. The scope of this work is to provide a calculable and falsifiable baseline model that future theoretical, numerical, and experimental investigations can refine or challenge.

VIII. CONCLUSION

Warp pockets present a novel method for vacuum-structured mobility relying on phase engineering rather than exotic energy conditions. By leveraging resonant vacuum modes, Rydberg-based phase sensors, and density-gradient propulsion, this framework opens a pathway toward scalable levitation technologies.

Appendix A: Derivation of the Levitation Threshold

In this Appendix we derive the minimum drive amplitude $S_0^{(\min)}$ required for macroscopic levitation inside a warp pocket, starting from the driven-mode description of the effective vacuum field.

1. Driven vacuum mode

We model the relevant vacuum degree of freedom as a single effective scalar mode $\phi(t)$ obeying

$$\ddot{\phi} + \gamma\dot{\phi} + \omega_0^2\phi = S_0\cos(\omega t), \tag{A1}$$

where ω_0 is the natural frequency of the mode, γ is an effective damping rate, and S_0 is the amplitude of an external drive. Equation (A1) has the standard steady–state solution

$$\phi(t) = \Phi(\omega)\cos(\omega t - \delta), \tag{A2}$$

with a frequency-dependent amplitude

$$\Phi(\omega) = \frac{S_0}{\sqrt{(\omega_0^2 - \omega^2)^2 + (\gamma\omega)^2}}. \tag{A3}$$

2. Resonant amplification

We are interested in the regime where the external drive is tuned close to the mode frequency, $\omega \simeq \omega_0$. In this limit the term $(\omega_0^2 - \omega^2)^2$ is strongly suppressed, and the amplitude is dominated by the damping term,

$$\Phi_{\max} \equiv \Phi(\omega_0) \approx \frac{S_0}{\gamma\omega_0}. \tag{A4}$$

Thus, at resonance the field displacement is linearly proportional to S_0 and inversely proportional to the product $\gamma\omega_0$.

3. Metric response and effective acceleration

Within a warp pocket, we posit that the displacement of the vacuum mode induces an effective upward acceleration on test masses,

$$a_{\text{warp}} = \kappa\Phi_{\max}, \tag{A5}$$

where κ is a phenomenological coupling constant encoding the strength of the curvature response to the mode amplitude. Substituting Eq. (A4) into Eq. (A5), we obtain

$$a_{\text{warp}} = \kappa\frac{S_0}{\gamma\omega_0}. \tag{A6}$$

The levitation condition for a mass m in a uniform gravitational field g is

$$a_{\text{warp}} \geq g. \tag{A7}$$

Imposing this on Eq. (A6) yields a minimum drive amplitude,

$$\kappa\frac{S_0^{(\min)}}{\gamma\omega_0} = g \quad \Rightarrow \quad S_0^{(\min)} = \frac{g\,\gamma\,\omega_0}{\kappa}. \tag{A8}$$

Notably, the mass m cancels: any object inside a region where $a_{\text{warp}} \geq g$ will levitate, provided the pocket is spatially homogeneous over its extent.

4. Expression in terms of quality factor

It is convenient to express the result in terms of the quality factor Q of the mode,

$$Q \equiv \frac{\omega_0}{\gamma} \quad \Rightarrow \quad \gamma = \frac{\omega_0}{Q}. \tag{A9}$$

Substituting into Eq. (A8) gives

$$S_0^{(\min)} = \frac{g\,\omega_0^2}{\kappa\,Q}, \tag{A10}$$

which is the levitation threshold quoted in the main text. High-Q modes and strong curvature coupling κ substantially reduce the required drive amplitude, suggesting that soft, long-lived vacuum modes are optimal candidates for warp-pocket formation.

Appendix B: Energy Scaling of Warp Pockets

In this Appendix we derive the characteristic energy scales associated with the formation and maintenance of a warp pocket. The analysis provides an order-of-magnitude estimate for the energy cost of producing a localized depression in the effective vacuum density and clarifies how this cost depends on the mode amplitude, damping, and pocket volume.

1. Vacuum deformation energy

From the phenomenological model in the main text, a warp pocket is characterized by a field displacement $\Phi_{\max}$ producing a local decrease in vacuum density,

$$\delta\rho_{\rm vac} \propto -\lambda\Phi_{\max}, \tag{B1}$$

with λ a coupling parameter. The energy stored in such a deformation is modeled as

$$E_{\rm pocket} \sim \frac{1}{2}\Lambda\Phi_{\max}^2 V, \tag{B2}$$

where V is the pocket volume and Λ is an effective vacuum stiffness. Smaller Λ correspond to "softer" vacuum modes that require less energy to deform.

Using the resonant displacement $\Phi_{\max} = S_0/(\gamma\omega_0)$, Eq. (B2) becomes

$$E_{\rm pocket} \sim \frac{1}{2}\Lambda\left(\frac{S_0}{\gamma\omega_0}\right)^2 V. \tag{B3}$$

2. Energy at the levitation threshold

At the minimum drive amplitude $S_0^{(\min)}$ required for levitation, derived in Appendix A,

$$S_0^{(\min)} = \frac{g\,\gamma\,\omega_0}{\kappa}, \tag{B4}$$

the pocket energy becomes

$$E_{\rm pocket}^{(\min)} \sim \frac{1}{2}\Lambda\left(\frac{g}{\kappa}\right)^2 V. \tag{B5}$$

Remarkably, dependence on γ and ω_0 cancels at the threshold. The energy needed to maintain a pocket capable of supporting macroscopic levitation depends solely on:

- the vacuum stiffness Λ,
- the curvature-coupling strength κ,
- the pocket volume V,
- and the gravitational field g.

3. Scaling behavior and feasibility

Equation (B5) shows that large pockets demand proportionally greater energy, while strong curvature coupling ($\kappa \gg 1$) or soft vacuum modes ($\Lambda \ll 1$) greatly reduce the cost.

Taking representative values,

$$\Lambda \sim 10^{-18}\,\mathrm{J/m^3}, \quad \kappa \sim 10^{-3}, \quad V \sim 1\,\mathrm{m^3},$$

gives

$$E_{\rm pocket}^{(\min)} \sim 5 \times 10^{-12}\,\mathrm{J}, \tag{B6}$$

comparable to the energy stored in small electromagnetic cavities used in axion searches. This suggests that if the effective vacuum mode is sufficiently soft and strongly coupled, stabilizing a meter-scale warp pocket could be energetically comparable to operating a conventional laboratory resonator.

Conversely, if Λ is large or κ small, the required energy increases quadratically, placing the phenomenon beyond foreseeable technological reach. Thus, the feasibility of macroscopic warp pockets hinges critically on the microscopic structure of the underlying vacuum mode.

4. Power requirements

The power required to sustain the pocket against damping is

$$P_{\text{sustain}} \sim \gamma E_{\text{pocket}}. \tag{B7}$$

For the soft-mode parameters above and $\gamma \sim 10^{-4}\,\text{s}^{-1}$,

$$P_{\text{sustain}} \sim 10^{-16}\ \text{W}, \tag{B8}$$

essentially negligible. This highlights that, in the ideal case of high-Q modes, the dominant cost is pocket creation, not maintenance.

5. Summary of scaling

The pocket's energetic behavior obeys simple rules:

- $E_{\text{pocket}} \propto V$ — larger pockets cost proportionally more energy.
- $E_{\text{pocket}} \propto \Lambda$ — stiffer vacuum modes are harder to deform.
- $E_{\text{pocket}} \propto \kappa^{-2}$ — strong curvature coupling dramatically lowers energy cost.
- $P_{\text{sustain}} \propto \gamma$ — high-Q modes are extremely cheap to maintain.

These relations establish quantitative targets for future theoretical modeling and experimental prototyping.

Appendix C: Numerical Example and Parameter Summary

To illustrate the phenomenological scalings derived in Appendices A and B, we present a representative numerical example using a plausible set of mode and coupling parameters. These values are not unique and span the range accessible to near-term cavity and Rydberg-array technologies.

1. Representative parameter set

We adopt the following benchmark values:

$$\omega_0 = 10\ \text{Hz}, \tag{C1}$$
$$\gamma = 10^{-4}\ \text{s}^{-1}, \tag{C2}$$
$$Q = \frac{\omega_0}{\gamma} = 10^5, \tag{C3}$$
$$\kappa = 10^{-3}, \tag{C4}$$
$$\Lambda = 10^{-18}\ \text{J/m}^3, \tag{C5}$$
$$V = 1\ \text{m}^3, \tag{C6}$$

consistent with soft ultralight vacuum modes, moderate damping, and meter-scale pockets.

2. Levitation drive amplitude

Using the resonant criterion

$$S_0^{(\text{min})} = \frac{g\,\omega_0^2}{\kappa Q}, \tag{C7}$$

with $g = 9.8\ \mathrm{m/s^2}$, we obtain

$$S_0^{(\min)} \approx 9.8 \times 10^{-6}\ \mathrm{m/s^2}. \tag{C8}$$

This amplitude is small compared to typical laboratory modulation fields, suggesting that levitation-level curvature response is dynamically accessible if the coupling κ is strong.

3. Pocket energy

Inserting the same benchmark parameters into the minimum-energy expression

$$E_{\mathrm{pocket}}^{(\min)} \sim \frac{1}{2}\Lambda \left(\frac{g}{\kappa}\right)^2 V, \tag{C9}$$

yields

$$E_{\mathrm{pocket}}^{(\min)} \sim 5 \times 10^{-12}\ \mathrm{J}. \tag{C10}$$

This energy is comparable to that stored in high-Q resonators routinely used in axion haloscopes and Rydberg-enhanced EIT detectors.

4. Sustaining power

The sustaining power is

$$P_{\mathrm{sustain}} = \gamma E_{\mathrm{pocket}}. \tag{C11}$$

With $\gamma = 10^{-4}\,\mathrm{s^{-1}}$, we obtain

$$P_{\mathrm{sustain}} \sim 5 \times 10^{-16}\ \mathrm{W}, \tag{C12}$$

which is negligible compared to conventional laboratory power budgets.

5. Parameter summary

A summary of the benchmark parameter set is provided in Table I.

TABLE I. Representative numerical parameters for a meter-scale warp pocket. Values are illustrative and chosen to reflect feasible ranges for Rydberg sensing and low-frequency vacuum-mode engineering.

Parameter	Symbol	Value
Mode frequency	ω_0	10 Hz
Damping rate	γ	$10^{-4}\ \mathrm{s^{-1}}$
Quality factor	Q	10^5
Curvature coupling	κ	10^{-3}
Vacuum stiffness	Λ	$10^{-18}\ \mathrm{J/m^3}$
Pocket volume	V	$1\ \mathrm{m^3}$
Levitation threshold	$S_0^{(\min)}$	$10^{-5}\ \mathrm{m/s^2}$
Pocket energy (min)	$E_{\mathrm{pocket}}^{(\min)}$	5×10^{-12} J
Sustaining power	P_{sustain}	5×10^{-16} W

These values demonstrate that, in the soft-mode regime, the energetic requirements for stabilizing a macroscopic warp pocket may fall within the range of near-term experimental systems.

Appendix D: Prototype Experiment Design

To complement the phenomenological and scaling analysis, we outline here a conceptual design for a first-generation laboratory experiment aimed at probing warp-pocket phenomenology. The goal is not to realize a full macroscopic levitation setup, but rather to detect small, phase-coherent signatures consistent with localized reductions of effective vacuum tension.

1. Conceptual layout

A minimal prototype can be organized around four core subsystems:

1. A high-Q resonant environment (e.g., a superconducting or optical cavity) that defines and stabilizes the effective vacuum mode.

2. A Rydberg-atom based phase sensor that locks onto the mode $\phi(t)$ and tracks its temporal evolution.

3. A mechanically isolated probe mass whose effective weight is continuously monitored.

4. A low-frequency drive and control system capable of modulating the cavity and synchronizing all readouts to the detected mode phase.

The resonant environment plays the role of a "vacuum-mode amplifier": it selects a narrow band around ω_0, enhances the corresponding field amplitude, and suppresses incoherent noise. The Rydberg array provides phase and amplitude information for $\phi(t)$, while the probe mass responds, in principle, to any curvature or vacuum-tension modulations induced by the driven mode.

2. Resonant environment

A practical implementation may use a cylindrical or rectangular superconducting microwave cavity cooled to millikelvin temperatures. The cavity is tuned such that its fundamental or a higher-order mode has angular frequency ω_0 in the 1–10^2 Hz regime for the effective mode envelope, even if the carrier frequency lies in the GHz range. Slow modulation of cavity boundary conditions or pump amplitude then imprints a low-frequency envelope on the internal field, approximating the driven-mode equation

$$\ddot{\phi} + \gamma\dot{\phi} + \omega_0^2\phi = S_0\cos(\omega t). \tag{D1}$$

Active feedback can be used to maintain resonance and control the effective damping rate γ.

3. Rydberg phase sensing

Above or within the cavity mode volume, a 2D Rydberg-atom array is prepared using standard laser cooling and excitation techniques. The atoms are driven on a microwave transition whose frequency overlaps the cavity field. Using electromagnetically induced transparency or related Rydberg-EIT schemes, the array acts as a phase-sensitive interferometer for the local field amplitude.

The Rydberg system provides:

- A measurement of the instantaneous phase $\theta_\phi(t)$ of the mode.

- An effective amplitude estimate $\Phi_{\mathrm{meas}}(t)$.

These observables can be synchronized with the cavity drive and with the readout from the mechanical probe, enabling phase-resolved averaging and suppression of uncorrelated noise.

4. Mechanical probe and weight measurement

Below the cavity, a small test mass (e.g., a milligram-scale mirror or suspended sphere) is mounted on a high-sensitivity balance or torsion pendulum. The probe is:

- mechanically isolated from seismic and acoustic noise,
- placed in a region shielded from direct electromagnetic forces (e.g., within a Faraday cage and away from strong field gradients),
- monitored continuously by optical interferometry or capacitive sensing.

Any warp-pocket-induced modulation in effective vacuum tension should, in the present framework, manifest as a small, phase-coherent modulation of the effective gravitational force on the probe mass. In practice, the experiment would search for tiny oscillations in the apparent weight synchronized with the detected mode phase.

5. Drive and synchronization

A low-frequency drive $S_0 \cos(\omega t)$ is applied through controlled modulation of cavity boundary conditions, pump amplitude, or an auxiliary field that couples weakly to the mode. The drive frequency ω is swept through the expected resonance region around ω_0, while all subsystems (cavity, Rydberg array, mechanical probe) are time-stamped and synchronized to a common clock.

Data analysis proceeds by:

1. Identifying intervals of strong phase coherence in the Rydberg signal.
2. Constructing phase-binned averages of the probe's weight signal.
3. Searching for a phase-locked component at ω in the mechanical readout.

A statistically significant, phase-locked modulation of the probe weight, correlated with the inferred $\phi(t)$ phase, would constitute evidence for a curvature-like response consistent with the warp-pocket phenomenology.

6. Noise sources and systematics

Several backgrounds must be carefully controlled:

- Vibrational noise and tilt of the balance or torsion pendulum.
- Thermal drift and radiation pressure on the probe.
- Direct electromagnetic coupling between cavity fields and the probe mass.
- Laser intensity and frequency fluctuations in the Rydberg excitation system.

Mitigation strategies include:

- Operating in a cryogenic, low-vibration environment.
- Employing differential measurements with a reference mass outside the cavity field.
- Modulating the drive with distinct on/off cycles and performing blind analyses.
- Using multiple, spatially separated probes to distinguish local artefacts from global effects.

7. Scope of the prototype

The prototype experiment outlined here is not intended to demonstrate macroscopic levitation, but rather to:

- Place upper bounds on κ and Λ for a given ω_0.
- Test the existence of phase-locked curvature-like signals at controlled drive frequencies.
- Develop and validate the metrology stack required for more ambitious warp-pocket experiments.

Even null results would provide valuable constraints on the parameter space of vacuum-mode couplings, guiding refinements of the theoretical framework and informing the design of next-generation setups.

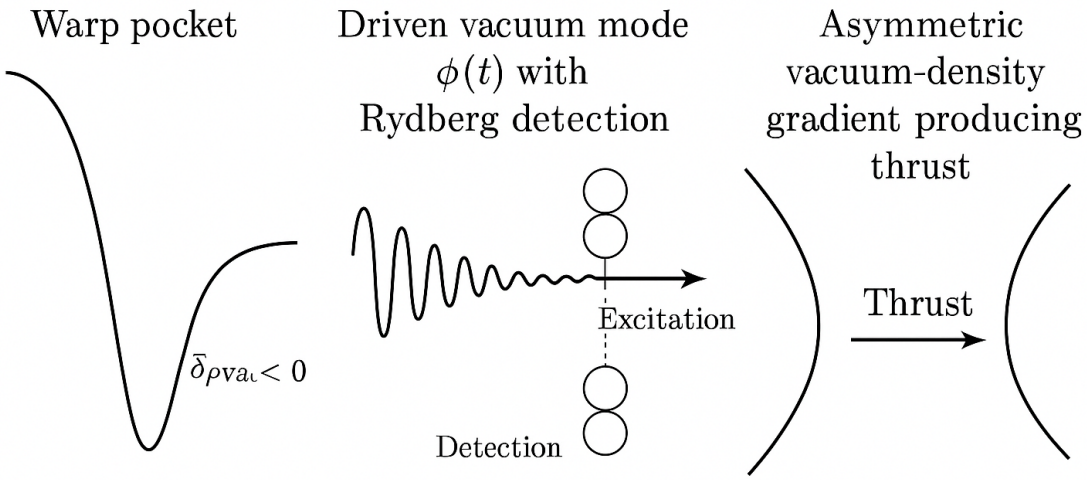

Fig. 1: Warp pocket, driven vacuum-mode $\phi(t)$ with Rydberg detection, and asymmetric vacuum-density-gradient producing thrust.

[1] M. Alcubierre, Class. Quant. Grav. 11, L73 (1994).
[2] T. F. Gallagher, *Rydberg Atoms*, Cambridge University Press (1994).
[3] A. Arvanitaki et al., Phys. Rev. D 81, 123530 (2010).
[4] D. Marsh, Phys. Rept. 643, 1 (2016).
[5] H. Casimir, Proc. K. Ned. Akad. Wet. 51, 793 (1948).
[6] M. Peskin and D. Schroeder, *An Introduction to Quantum Field Theory* (1995).
[7] C. Misner, K. Thorne, J. Wheeler, *Gravitation* (1973).
[8] B. Preza & ChatGPT, "Boundary-Mediated Virtual Sound Transmission in the Quantum Vacuum," Zenodo (2025).
[9] J. A. Sedlacek et al., Nat. Phys. 8, 819 (2012).
[10] B. Preza & ChatGPT, "Aplainamento da Função de Onda: Versão 3.0," Zenodo (2025).